

Free-free background radiation from accreting primordial black holes

Hiroyuki Tashiro,* Katsuya T. Abe, and Teppei Minoda

Division of Particle and Astrophysical Science, Graduate School of Science,

Nagoya University, Chikusa, Nagoya 464-8602, Japan

(Dated: June 13, 2022)

Baryonic gas falling onto a primordial black hole (PBH) emits photons via the free-free process. These photons can contribute the diffuse free-free background radiation in the frequency range of the cosmic microwave background radiation (CMB). We show that the intensity of the free-free background radiation from PBHs depends on the mass and abundance of PBHs. In particular, considering the growth of a dark matter (DM) halo around a PBH by non-PBH DM particles strongly enhances the free-free background radiation. This enhancement allows us to obtain the tight constraint on the PBH abundance with mass $M_{\text{PBH}} > 10M_{\odot}$. Comparison with the CMB free-free foreground component in high galactic latitude measured by Planck, our constraint on the PBH abundance fraction to the total DM, f_{PBH} , is $f_{\text{PBH}} < 1.2 \times 10^{-5} (M_{\text{PBH}}/100M_{\odot})^{-2.3}$. We also discuss the impact of the free-free radiation from PBHs on the measurement of 21-cm background radiation from high redshifts, including the EDGES anomaly.

I. INTRODUCTION

The existence of dark matter (DM) is strongly supported by a variety of astrophysical and cosmological observations [1, 2]. The most explored candidate is new elementary particles beyond the standard model of particle physics, i.e., weakly interacted massive particle [3, 4]. Although many experiments have been conducted aggressively to study these candidates, the detection has not been reported yet.

A primordial black hole (PBH) is one of the viable candidates for non-particle DM. The original idea of PBH is advocated by Zel'dovich and Novikov in 1960 [5]. PBHs form from the gravitational collapse of the overdense regions in the early universe, and their mass is in a wide range from the Planck mass to masses much larger than the solar mass [6]. PBHs are considered to be a candidate of DM for a long time [7, 8]. Although, currently, there is no evidence for the existence of PBHs, the recent detections of gravitational waves by LIGO/VIRGO draw attention to PBHs [9]. From the existing constraints, PBHs with mass responsible for the above GW events with stellar-mass BH binary merger, cannot account for the total amount of DM. However, still, PBHs can be a subdominant component of DM [10, 11].

The stringent constraints on PBHs with mass $M \gtrsim \mathcal{O}(1)M_{\odot}$ have been obtained in the gas accretion scenario onto PBHs [12, 13]. PBH gravitational force attracts the surrounding gas. When accreting onto a PBH, gas is heated up and ionized enough to emit X-ray and UV photons by the free-free emission. These high energy photons can modify the thermal and ionization history of the diffuse background gas before the epoch of reionization. Since such modification affects the CMB anisotropies, CMB observations can provide the strong constraint on the amount of PBHs [13–15]. The measurement of these effects has been also discussed in the

Sunyaev-Zel'dovich effect fluctuations [16] and future 21-cm observations [17–20].

The free-free emission from accreting gas has a continuous spectrum below the UV frequency. Since these photons are not consumed for the heating and ionization of the background gas, we can observe this emission directly as diffuse background radiation. According to detailed studies in the CMB frequency range, the radiation with the free-free spectrum is in the order of several tens of μK and most of them are considered to be of Galactic origin [21, 22]. However, some fraction of them could be the contribution from large-scale structure or the structure formation in the early universe [23–26].

In this paper, we evaluate the intensity of the free-free background radiation from PBHs. By comparing it with the current observational data, we provide the constraint on the PBH abundance with stellar mass. Throughout this paper, we take the flat ΛCDM model with the cosmological parameters $(\Omega_m, \Omega_b, h) = (0.3, 0.05, 0.7)$.

II. FREE-FREE EMISSION AROUND A PBH

A PBH can accrete baryon gas after the matter-radiation equality. During the accretion, the gas is heated up and ionized. As a result, the accreting gas around a PBH can emit radiation via a free-free emission process. In order to evaluate this free-free emission, it is required to obtain the gas profile of the density, temperature, and ionization rate around a PBH. Recently Refs. [12, 13] have investigated the gas accretion onto a PBH in the cosmological context. Assuming the spherical accretion and the steady-state approximation, they have obtained a simple model of gas profile. In this section, following the procedure in Ref. [13], we evaluate the free-free emission from a PBH.

We consider the accretion gas onto a PBH with mass M_{PBH} at a redshift z . The simple spherical accretion can be described by the Bondi accretion [27]. Based on this model, we introduce the parameter λ describing the

* hiroyuki.tashiro@nagoya-u.jp

spherical accretion rate \dot{M} ,

$$\dot{M} = 4\pi\lambda\bar{\rho}_b r_B^2 c_s, \quad (1)$$

where $\bar{\rho}_b$ is the background baryon gas density, c_s is the sound velocity of the background baryon gas, and r_B is the Bondi radius, $r_B = GM_{\text{PBH}}/c_s^2$.

In the determination of the radial profiles of the accreting gas, one of the largest theoretical uncertainties is the ionization process of the gas. The gas ionization is accomplished through not only the collisional ionization but also photoionization by the emission from hot ionized gas in the central region. We assume that the gas is ionized only by the thermal collision ionization process. In this assumption, for simplicity, the ionization does not proceed until the temperature reaches the critical temperature $T_{\text{ion}} \sim 10^4$ K. When reaching the critical temperature, the ionization fraction would increase until $x_e = 1$ with keeping $T = T_{\text{ion}}$. This assumption provides the conservative estimation of the free-free emission [13].

Ref. [13] divides the radial gas profile into three regions; the outermost region, collisional ionization region, and innermost adiabatic region. In the outermost region, the gas density and the temperature increases from the background values, $\bar{\rho}_b$ and \bar{T} , as the radius, r , decreases. When the steady-state approximation is valid the spherical accreting gas can be described by the following equations,

$$4\pi r^2 \rho_b |v| = \dot{M}, \quad (2)$$

$$v \frac{dv}{dr} = -\frac{GM_{\text{PBH}}}{r^2} - \frac{1}{\rho_b} \frac{dP}{dr} - \frac{4}{3} \frac{\bar{x}_e \sigma_T \rho_{\text{CMB}}}{m_p c} v, \quad (3)$$

$$v \rho_b^{2/3} \frac{d}{dr} \left(\frac{T}{\rho_b^{2/3}} \right) = \frac{8\bar{x}_e \sigma_T \rho_{\text{CMB}}}{3m_e c (1 + \bar{x}_e)} (T_{\text{CMB}} - T), \quad (4)$$

where ρ_b is the gas energy density, $|v|$ is the gas radial velocity, P is the gas pressure, ρ_{CMB} is the CMB energy density, σ_T is the cross-section of the Thomson scattering, and \bar{x}_e is the background ionization rate. The first equation is the mass conservation equation, and the second and the third equations are the momentum equation and heat equation of gas, respectively. The last terms in Eqs (3) and (4) represent the Compton drag and cooling terms. They provide a significant impact on the accretion in high redshifts. It is useful to introduce two dimensionless parameters describing the time scales of these CMB effects,

$$\beta = \frac{4}{3} \frac{\bar{x}_e \sigma_T \rho_{\text{CMB}}}{m_p c} t_B, \quad \gamma = \frac{8\bar{x}_e \sigma_T \rho_{\text{CMB}}}{3m_e c (1 + \bar{x}_e)} t_B, \quad (5)$$

where t_B is the time scale of the Bondi accretion, $t_B = GM_{\text{PBH}}/c_s^3$.

Once λ is determined, the gas profiles in the outermost region are provided by Eqs. (2)-(4). Although the accretion rate depends on the physical condition around a PBH, Ref. [13] have found out λ which can provide the

physically valid solution of Eqs. (2)-(4). The approximated form of such λ is given by

$$\lambda(\gamma, \beta) = \frac{\lambda_{\text{ad}} + (\lambda_{\text{iso}} - \lambda_{\text{ad}}) \left(\frac{\gamma^2}{88 + \gamma^2} \right)^{0.22}}{(\sqrt{1 + \beta} + 1)^2} \exp \left[\frac{9/2}{3 + \beta^{3/4}} \right], \quad (6)$$

where $\lambda_{\text{ad}} = (3/5)^{3/2}/4$ and $\lambda_{\text{iso}} = e^{3/2}/4$. In this case, following Eqs. (2)-(4), the gas density and the temperature are proportional to $T \propto \rho^{2/3} \propto 1/r$, respectively. The smallest radius of the outermost region is r_i where the temperature reaches $T = T_{\text{ion}}$. The radius r_i is $r_i \approx f T_{\text{CMB}} r_B / T_{\text{ion}}$, where f the coefficient of 0.3 which can be smaller when Compton cooling is effective.

Inside $r < r_i$, the collisional ionization becomes effective. In this collisional ionization region, as we mentioned above, the gas keeps the temperature, T_{ion} , with increasing the ionization fraction. However, since the gas suffers the adiabatic compression, the gas density follows $\rho \propto r^{-3/2}$. Then, the ionization fraction is given in $(1 + x_e) \propto r^{-1/8}$ [13]. The radius where $x_e = 1$ is provided in $r_e = (1 + \bar{x}_e)^8 r_i / 2^8$.

In the innermost adiabatic region, $r < r_e$, the gas density and temperature follow the adiabatic compression. The gas density and the temperature are proportional to $\propto r^{-2/3}$ and r^{-1} , respectively. When the temperature exceeds the electron mass, relativistic correction is required. As a result, the temperature profile is modified to $T \propto r^{-2/3}$ in the region where $T > m_e c^2$. The accretion flow reaches the Schwarzschild radius, r_S , and the gas velocity becomes almost the speed of light. At r_S , the temperature of gas reaches $T \sim 10^9$ K.

So far we consider the spherical Bondi accretion. However, there exists the relative velocity between DM and baryons. The coherent scale of the velocity is several comoving Mpc. The amplitude is larger than the sound speed of baryon gas soon after the recombination epoch, $\langle v_L^2 \rangle \approx \min[1, z/10^3] \times 30$ km/s as shown in Ref. [28]. Due to this relative velocity, the spherically accretion model must be corrected. Ref. [13] proposed the replacement of c_s in the above discussion to

$$v_{\text{eff}} \approx \begin{cases} \sqrt{v_B \langle v_L^2 \rangle^{1/2}}, & v_B \ll \langle v_L^2 \rangle^{1/2}, \\ v_B, & v_B \gg \langle v_L^2 \rangle^{1/2}. \end{cases} \quad (7)$$

Following this procedure, we calculate the radial profile in the subsequent sections.

Although we consider the accretion of baryon gas onto PBHs, due to the gravity of a PBH, non-PBH DM particles also accrete on the PBH, and a DM halo forms around the PBH. The created PBH halo enhances the accretion of baryons onto PBHs and, resultantly, amplifies the free-free emission. In order to include this effect, we adopt the simple semi-analytical model provided in Ref. [15]. In this model, the DM halo mass M_{halo} grows as $M_{\text{halo}} \propto (1+z)$ after the matter-radiation equality suggested in Ref. [29]. Fig. 1 shows the enhancement of the accretion rate by considering the DM halo effect. In this

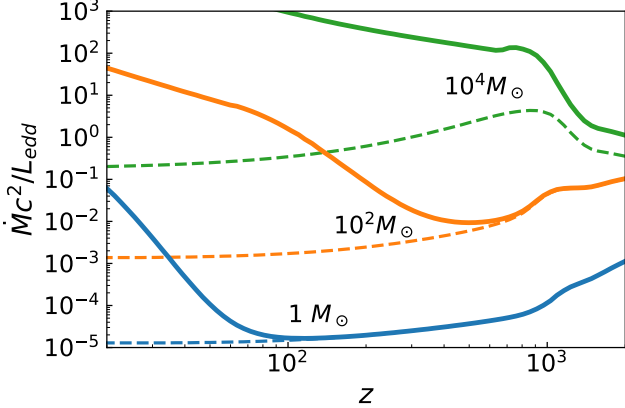


FIG. 1. Accretion rate normalized in the Eddington luminosity. The solid lines are with the DM halo effect while the dashed lines are without the DM halo effect. From top to bottom, the lines represents for $M_{\text{PBH}} = 10^4, 10^2$ and $1 M_\odot$.

plot, we normalize the mass accretion to the Eddington luminosity. The solid lines represent the ones with the DM halo effect while the dashed lines are without the DM halo effect. The DM halo enhancement is prominent in lower redshifts. For example, in $z \approx 30$, the total mass gravitationally attracting the baryon gas in the outermost region becomes 100 times larger than the initial mass of the central PBH. In lower redshifts, the gravity of growing DM halos dominates the PBH and strongly enhances the accretion of baryon gas. The gas falling into a PBH increases the mass of the PBH. We calculate the increment of the PBH mass after the matter-radiation equality, $\Delta M(z) = \int_{t_{\text{eq}}}^{t(z)} \dot{M} dt$. Because of the accretion, the PBH mass rapidly increases in low redshifts. As the initial PBH is massive, the accreted mass grows PBH mass more. The growth of the PBH mass increases the Schwarzschild radius more than the initial one. However, this increase does not modify our final result for the PBH mass less than $10^4 M_\odot$.

III. DIFFUSE FREE-FREE BACKGROUND RADIATION

Ionized hot accreting gas can emit radiation via free-free emission. First, we evaluate the intensity of the free-free emission from an individual PBH.

Now we consider a line of sight with impact parameter b in unit of r from the center of the PBH. The intensity of the free-free emission at a frequency ν is calculated by the integration over this line of sight

$$I_\nu(b) = \int_{-R_{\text{max}}}^{R_{\text{max}}} f_\nu(R) j_\nu(\ell) dR, \quad (8)$$

where R is the position along the line of sight, and $R = 0$ represents the center of this line of sight in the accreting

gas. The radial distance ℓ satisfies $\ell^2 = R^2 + (br_s)^2$, and R_{max} is given by $R_{\text{max}} = \sqrt{1 - b^2} r_s$. The function $f_\nu(R)$ is given by

$$f_\nu(R) = \exp[-(\tau_\nu(R_{\text{max}}) - \tau_\nu(R))], \quad (9)$$

where the optical depth $\tau_\nu(R)$ at the frequency ν is obtained from

$$\tau_\nu(R) = \int_{-R_{\text{max}}}^R \alpha_\nu(\ell) dR, \quad (10)$$

with the absorption coefficient α_ν .

The radial profiles of the emission and absorption coefficients are given by [30]

$$j_\nu(r) = \frac{2^3 e^6}{3m_e c^3} \sqrt{\frac{2\pi}{3k_B T m_e}} n_e n_p \bar{g}_{\text{ff}}, \quad (11)$$

$$\alpha_\nu(r) = \frac{4e^6}{3m_e c k_B T} \sqrt{\frac{2\pi}{3k_B T m_e}} n_e n_p \bar{g}_{\text{ff}}, \quad (12)$$

where e is the electric charge, and \bar{g}_{ff} is the velocity averaged Gaunt factor. We adopt the approximation form in Ref. [31],

$$\bar{g}_{\text{ff}} = \log \left\{ \exp \left[5.960 - \sqrt{3}/\pi \log \left(\nu_9 T_4^{-3/2} \right) \right] + e \right\}, \quad (13)$$

where $\nu_9 \equiv \nu/(1 \text{ GHz})$, $T_4 \equiv T/(10^4 \text{ K})$ and e is the Napier's constant. When the frequency is much smaller than $k_B T/h$ and the absorption is negligible, the frequency dependence comes from only \bar{g}_{ff} , and its dependency on the frequency is very weak. As a result, the free-free intensity is almost scale-invariant, $I \propto \nu^{-0.1}$.

The intensity averaged over the cross-section is

$$\bar{I}(\nu) = \int_0^1 I_\nu(b) b db. \quad (14)$$

Since the radial profile of gas around a PBH depends on the redshift z , the averaged intensity is also a function of z . Hereafter we represent it as $\bar{I}(\nu, z)$.

The intensity averaged over the full sky is obtained by taking into account PBHs with the comoving number density n_{PBH} ,

$$I_{\text{PBH}}(\nu_{\text{obs}}) = \frac{1}{4\pi} \int_{z_c}^{\infty} \frac{\bar{I}(\nu_z, z)}{(1+z)^3} \Delta\Omega(z) n_{\text{PBH}} \frac{dV_c}{dz} dz, \quad (15)$$

where $\nu_z = (1+z)\nu_{\text{obs}}$, $\Delta\Omega(z)$ is the solid angle of a PBH at z , $\Delta\Omega = \pi(1+z)r_s^2/D^2(z)$ with the comoving distance $D(z)$, and V_c is the comoving volume of the Universe at the redshift z . In the equation, z_c is the lower limit of the redshift integration. Although we assume the adiabatic evolution of the background gas temperature, stars and galaxies can heat up it in lower redshift. The heated gas temperature suppresses the accretion rate. The impact of the star and galaxy formation on the gas temperature evolution is still unknown. In order to avoid this model

uncertainty, we set $z_c = 20$ in this paper. Eq. (15) tells us that the free-free emission intensity is proportional to f_{PBH} , because the comoving number density n_{PBH} is $n_{\text{PBH}} = f_{\text{PBH}}\Omega_{\text{DM}}\rho_c/M_{\text{PBH}}$. When the optically thin approximation is valid (the absorption contribution can be negligible), Eq. (15) is approximated to

$$I_{\text{PBH}}(\nu_{\text{obs}}) \approx \int \frac{\bar{j}(\nu_z, z)}{(1+z)^4} \frac{dD(z)}{dz} dz, \quad (16)$$

where \bar{j} is given by

$$\bar{j}(\nu, z) = (1+z)^3 n_{\text{PBH}} \int_0^{r_s} j_\nu(r) 4\pi r^2 dr. \quad (17)$$

IV. CONSTRAINT ON THE PBH ABUNDANCE

The free-free emission has an almost-flat frequency spectrum as mentioned in the previous section. In the CMB frequency range, such frequency-invariant free-free emission is well studied as one of the main foreground sources [22].

We calculate the free-free emission induced by PBHs at the CMB frequency range. Fig. 2 shows the emission intensity at the observation frequency, $\nu_{\text{obs}} = 44$ GHz. Evaluating the intensity for the different M_{PBH} , we found that the intensity with the DM halo effect is fitted as

$$I_{\text{PBH}} \approx 4.1 \times 10^3 \left(\frac{f_{\text{PBH}}}{10^{-3}} \right) \left(\frac{M_{\text{PBH}}}{100 M_\odot} \right)^{2.3} \text{ Jy/str}, \quad (18)$$

for $M_{\text{PBH}} > 10 M_\odot$. For PBHs with $M_{\text{PBH}} < 10 M_\odot$, the enhancement of the DM accretion is ineffective. In particular, when $M_{\text{PBH}} < 0.1 M_\odot$, the intensity of the free-free emission with the DM halo effect is same as the one without the DM halo effect, $I_{\text{PBH}} \approx 3.6 \times 10^{-3} (f_{\text{PBH}}/10^{-3}) (M_{\text{PBH}}/100 M_\odot)^{2.3}$ Jy/str.

In the analysis for the foreground radiation in the CMB frequency range with the Planck data, Ref. [22] identified the free-free emission component as $I_{\text{ff}} \approx 2000$ Jy/str ($T_{\text{b,ff}} \approx 35 (\nu_{\text{obs}}/44 \text{ GHz})^{-2} \mu\text{K}$ in terms of the brightness temperature, T_{b}). This is consistent with the results in ARCADE 2 [32]. Since the free-free emission from PBHs cannot exceed this value, we can obtain the constraint on f_{PBH} . We plot the constraint on f_{PBH} as the green solid line in Fig. 3. For comparison, we show the constraint from the CMB anisotropy in Ref. [15]. The DM halo effect amplifies the mass for attracting the accreting gas by a factor of 100 in lower redshifts. Therefore, the case with including the DM halo effect provides the stronger constraint (the orange solid line in Fig. 3) which is approximately expressed for $M_{\text{PBH}} > 10 M_\odot$ in

$$f_{\text{PBH}} < 4.9 \times 10^{-4} \left(\frac{M_{\text{PBH}}}{100 M_\odot} \right)^{-2.3}. \quad (19)$$

In the Planck analysis, the observed free-free emission is strongly anisotropic [22]. The strong emission comes

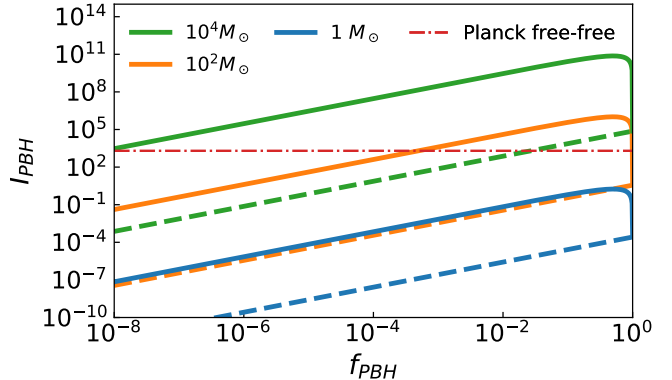


FIG. 2. Intensity of the diffuse free-free background radiation from PBHs. The solid and the dashed lines are for the intensity with and without the DM halo effect, respectively. The different colors mean different PBH masses. The dotted-dashed line represents the intensity of the diffuse free-free component measured by Planck.

from the region in low galactic latitude while the signals become much lower in high galactic latitude. Using the Planck free-free emission map, Ref. [26] evaluated that the free-free emission in high galactic latitude $|b| > 60$, $I_{\text{ff}} \sim 60$ Jy/str in the CMB frequency range. When we apply this value, the constraint becomes much tighter as represented as the dashed orange and green lines in Fig. 3. In particular, the constraint with the DM effect is approximately given for $M_{\text{PBH}} > 10 M_\odot$ in

$$f_{\text{PBH}} < 1.2 \times 10^{-5} \left(\frac{M_{\text{PBH}}}{100 M_\odot} \right)^{-2.3}. \quad (20)$$

This constraint is stronger than the one from the CMB anisotropy analysis.

Application to the global 21-cm signals

The free-free emission from PBHs has a flat frequency spectrum. Although in the CMB frequency range, the spectrum is much lower than the CMB blackbody spectrum, it could exceed the CMB spectrum in the lower frequency range. Therefore, depending on f_{PBH} and M_{PBH} , the free-free emission from PBHs could become a major background radiation source in low frequencies. Such background radiation excess enhances the absorption feature of the global 21-cm signal in the dark ages and cosmic dawn [33].

Recently, the EDGES collaboration has reported the larger absorption signals of redshifted 21-cm lines between redshift $z = 20$ and $z = 15$ [34]. The observed absorption is two times stronger than the maximum value in the predictions with the standard cosmological model.

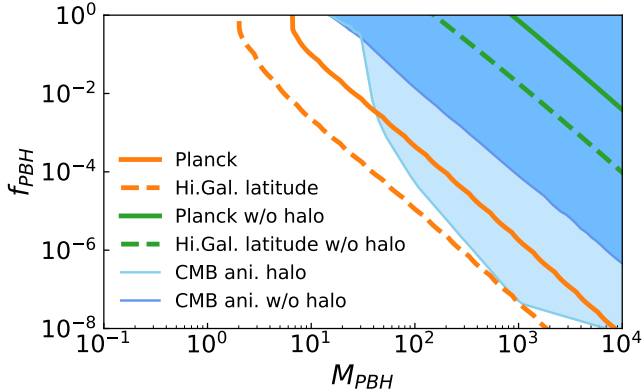


FIG. 3. Constraint on the PBH abundance from the free-free emission. The solid lines represent the constraint from the Planck foreground analysis. The dashed lines show the constraints from the free-free emission in high galactic latitude. The orange and green lines are for the intensities with and without the DM halo effect, respectively. The blue hatched regions show the parameter regions excluded by the Planck CMB anisotropy [15].

We calculate the brightness temperature of the free-free emission from PBHs at 1420 MHz in the redshift $z = 15$,

$$T_{b,\text{PBH}} \approx 3.1 \left(\frac{f_{\text{PBH}}}{10^{-4}} \right) \left(\frac{M_{\text{PBH}}}{100 M_{\odot}} \right)^{2.3} \text{ K.} \quad (21)$$

The required brightness temperature of the free-free emission to explain the EDGES anomaly depends on the gas temperature and the strength of the Lyman- α background radiation. In the simple case, where gas is adiabatically cooled and there exists strong Lyman- α background from stars, the required brightness temperature is twice the CMB temperature. Therefore, the free-free emission from PBHs can create enough brightness temperature of the background radiation with f_{PBH} which is consistent with our constraint in Eq. (19). In other words, $f_{\text{PBH}} \gtrsim 0.67 \times 10^{-4} (M_{\text{PBH}}/100 M_{\odot})^{-2.3}$ produces deeper absorption than the EDGES signals.

V. CONCLUSION

PBHs accrete the baryon gas by their gravity. The accreting gas is heated up and ionized due to the com-

pression during the accretion. Such hot ionized gas can emit free-free emissions, and the sum of these emissions contributes to the diffuse free-free background radiation. In this paper, we have calculated the intensity of the free-free background radiation and obtained the relation between the intensity and the PBH abundance. We have found that considering the growth of the DM halo around a PBH enhances the free-free emission strongly. Because of the DM growth, the emission contribution from lower redshifts dominates the one from higher redshifts.

Comparing with the diffuse free-free component measured in the CMB frequency, we obtain the constraint on the PBH abundance for stellar-mass PBHs. Without the DM halo growth, the constraint is much weaker than the current constraint from the CMB anisotropy. However, including the DM halo growth improves the constraint. The comparison with the free-free emission in high galactic latitude can yield a stronger constraint than in the previous works.

The free-free background radiation from PBHs can enhance the absorption feature of the 21-cm signals, and it may help to explain the EDGES anomaly. We have evaluated the brightness temperature at the 21-cm frequency in the EDGES redshift range. We have shown that the free-free emission can produce radiation whose brightness temperature is larger than twice the CMB temperature required to explain the EDGES anomaly. Ref. [19] has already studied the constraint on the PBH abundance based on the EDGES report. However, they do not consider the free-free emission as the background radiation. Our results tell us that the free-free emission cannot be negligible when the DM halo effect is negligible. We will revisit the implication of the PBH constraint from the EDGES report in the next paper.

There is the possibility that the stellar mass and massive PBHs form the accretion disk [14]. The radiation from the disk can be stronger than in the spherical case as in this paper. However, when the radiation is strong, it induces the photoionization and heats up the gas in the cosmological scales [16, 17]. To evaluate these effects, a numerical simulation is required. We also leave them for our future work.

ACKNOWLEDGMENTS

This work is supported by Japan Society for the Promotion of Science (JSPS) KAKENHI Grants No. JP21K03533 (H.T) and No. JP20J22260 (K.T.A), and supported by JSPS Overseas Research Fellowships (T.M.).

[1] D. Clowe, M. Bradač, A. H. Gonzalez, M. Markevitch, S. W. Randall, C. Jones, and D. Zaritsky, A Direct Empirical Proof of the Existence of Dark Matter, *ApJ* **648**, L109 (2006), arXiv:astro-ph/0608407 [astro-ph].

[2] Planck Collaboration, Planck 2018 results. VI. Cosmological parameters, *A&A* **641**, A6 (2020), arXiv:1807.06209 [astro-ph.CO].

- [3] G. Jungman, M. Kamionkowski, and K. Griest, Supersymmetric dark matter, *Physics Reports* **267**, 195 (1996), arXiv:hep-ph/9506380 [hep-ph].
- [4] G. Bertone, D. Hooper, and J. Silk, Particle dark matter: evidence, candidates and constraints, *Physics Reports* **405**, 279 (2005), arXiv:hep-ph/0404175 [hep-ph].
- [5] Y. B. Zel'dovich and I. D. Novikov, The Hypothesis of Cores Retarded during Expansion and the Hot Cosmological Model, *Soviet Astronomy* **10**, 602 (1967).
- [6] S. Hawking, Gravitationally collapsed objects of very low mass, *MNRAS* **152**, 75 (1971).
- [7] B. J. Carr and S. W. Hawking, Black holes in the early Universe, *MNRAS* **168**, 399 (1974).
- [8] G. F. Chapline, Cosmological effects of primordial black holes, *Nature (London)* **253**, 251 (1975).
- [9] S. Bird, I. Cholis, J. B. Muñoz, Y. Ali-Haïmoud, M. Kamionkowski, E. D. Kovetz, A. Raccanelli, and A. G. Riess, Did LIGO Detect Dark Matter?, *Phys. Rev. Lett.* **116**, 201301 (2016), arXiv:1603.00464 [astro-ph.CO].
- [10] B. Carr and F. Kühnel, Primordial Black Holes as Dark Matter: Recent Developments, *Annual Review of Nuclear and Particle Science* **70**, 355 (2020), arXiv:2006.02838 [astro-ph.CO].
- [11] A. M. Green and B. J. Kavanagh, Primordial black holes as a dark matter candidate, *Journal of Physics G Nuclear Physics* **48**, 043001 (2021), arXiv:2007.10722 [astro-ph.CO].
- [12] M. Ricotti, J. P. Ostriker, and K. J. Mack, Effect of Primordial Black Holes on the Cosmic Microwave Background and Cosmological Parameter Estimates, *Astrophys. J.* **680**, 829 (2008), arXiv:0709.0524 [astro-ph].
- [13] Y. Ali-Haïmoud and M. Kamionkowski, Cosmic microwave background limits on accreting primordial black holes, *Phys. Rev. D* **95**, 043534 (2017), arXiv:1612.05644 [astro-ph.CO].
- [14] V. Poulin, P. D. Serpico, F. Calore, S. Clesse, and K. Kohri, CMB bounds on disk-accreting massive primordial black holes, *Phys. Rev. D* **96**, 083524 (2017), arXiv:1707.04206 [astro-ph.CO].
- [15] P. D. Serpico, V. Poulin, D. Inman, and K. Kohri, Cosmic microwave background bounds on primordial black holes including dark matter halo accretion, *Physical Review Research* **2**, 023204 (2020), arXiv:2002.10771 [astro-ph.CO].
- [16] K. T. Abe, H. Tashiro, and T. Tanaka, Thermal Sunyaev-Zel'dovich anisotropy due to primordial black holes, *Phys. Rev. D* **99**, 103519 (2019), arXiv:1901.06809 [astro-ph.CO].
- [17] H. Tashiro and N. Sugiyama, The effect of primordial black holes on 21-cm fluctuations, *MNRAS* **435**, 3001 (2013), arXiv:1207.6405 [astro-ph.CO].
- [18] J.-O. Gong and N. Kitajima, Small-scale structure and 21cm fluctuations by primordial black holes, *J. Cosmology Astropart. Phys.* **2017**, 017 (2017), arXiv:1704.04132 [astro-ph.CO].
- [19] A. Hektor, G. Hütsi, L. Marzola, M. Raidal, V. Vaskonen, and H. Veermäe, Constraining primordial black holes with the EDGES 21-cm absorption signal, *Phys. Rev. D* **98**, 023503 (2018), arXiv:1803.09697 [astro-ph.CO].
- [20] O. Mena, S. Palomares-Ruiz, P. Villanueva-Domingo, and S. J. Witte, Constraining the primordial black hole abundance with 21-cm cosmology, *Phys. Rev. D* **100**, 043540 (2019), arXiv:1906.07735 [astro-ph.CO].
- [21] M. Seiffert, D. J. Fixsen, A. Kogut, S. M. Levin, M. Limon, P. M. Lubin, P. Mirel, J. Singal, T. Villela, E. Wollack, and C. A. Wuensche, Interpretation of the ARCADE 2 Absolute Sky Brightness Measurement, *Astrophys. J.* **734**, 6 (2011).
- [22] Planck Collaboration, Planck 2015 results. X. Diffuse component separation: Foreground maps, *A&A* **594**, A10 (2016), arXiv:1502.01588 [astro-ph.CO].
- [23] A. Cooray and S. R. Furlanetto, Free-Free Emission at Low Radio Frequencies, *ApJ* **606**, L5 (2004), arXiv:astro-ph/0402239 [astro-ph].
- [24] P. P. Ponente, J. M. Diego, R. K. Sheth, C. Burigana, S. R. Knollmann, and Y. Ascasibar, The cosmological free-free signal from galaxy groups and clusters, *MNRAS* **410**, 2353 (2011), arXiv:1006.2243 [astro-ph.CO].
- [25] B. Liu, J. Jaacks, S. L. Finkelstein, and V. Bromm, Global radiation signature from early structure formation, *MNRAS* **486**, 3617 (2019), arXiv:1901.08994 [astro-ph.GA].
- [26] K. T. Abe, T. Minoda, and H. Tashiro, Constraint on the early-formed dark matter halos using the free-free emission in the Planck foreground analysis, arXiv e-prints , arXiv:2108.00621 (2021), arXiv:2108.00621 [astro-ph.CO].
- [27] H. Bondi, On spherically symmetrical accretion, *MNRAS* **112**, 195 (1952).
- [28] D. Tseliakhovich and C. Hirata, Relative velocity of dark matter and baryonic fluids and the formation of the first structures, *Phys. Rev. D* **82**, 083520 (2010), arXiv:1005.2416 [astro-ph.CO].
- [29] K. J. Mack, J. P. Ostriker, and M. Ricotti, Growth of Structure Seeded by Primordial Black Holes, *Astrophys. J.* **665**, 1277 (2007), arXiv:astro-ph/0608642 [astro-ph].
- [30] G. B. Rybicki and A. P. Lightman, Radiative Processes in Astrophysics, (1986).
- [31] B. T. Draine, Physics of the Interstellar and Intergalactic Medium, (2011).
- [32] D. J. Fixsen, A. Kogut, S. Levin, M. Limon, P. Lubin, P. Mirel, M. Seiffert, J. Singal, E. Wollack, T. Villela, and C. A. Wuensche, ARCADE 2 Measurement of the Absolute Sky Brightness at 3-90 GHz, *Astrophys. J.* **734**, 5 (2011), arXiv:0901.0555 [astro-ph.CO].
- [33] C. Feng and G. Holder, Enhanced Global Signal of Neutral Hydrogen Due to Excess Radiation at Cosmic Dawn, *ApJ* **858**, L17 (2018), arXiv:1802.07432 [astro-ph.CO].
- [34] J. D. Bowman, A. E. E. Rogers, R. A. Monsalve, T. J. Mozdzen, and N. Mahesh, An absorption profile centred at 78 megahertz in the sky-averaged spectrum, *Nature (London)* **555**, 67 (2018), arXiv:1810.05912 [astro-ph.CO].